NEURO-ONCOLOGY

Evaluation of diffusion parameters as early biomarkers of disease progression in glioblastoma multiforme[†]

Inas S. Khayal, Mei-Yin C. Polley, Llewellyn Jalbert, Adam Elkhaled, Susan M. Chang, Soonmee Cha, Nicholas A. Butowski, and Sarah J. Nelson

UCSF/UCB Joint Graduate Group in Bioengineering (I.S.K., S.J.N.), Surbeck Laboratory of Advanced Imaging, Department of Radiology and Biomedical Imaging (I.S.K., L.J., A.E., S.J.N.), and Departments of Neurological Surgery (M.C.P., S.M.C., N.A.B., S.C.), Radiology and Biomedical Imaging (S.C.), and Bioengineering and Therapeutic Sciences (S.J.N.), University of California–San Francisco, San Francisco, California

The purpose of this study was to evaluate diffusion parameters at pre-, mid-, and post-radiation therapy (RT) in contrast-enhancing and nonenhancing lesions of post-surgical glioblastoma multiforme patients treated with the standard of care RT concurrently with temozolomide (TMZ) followed by adjuvant TMZ and an antiangiogenic drug. The diffusion parameters explored include baseline and short-term changes in apparent diffusion coefficient, fractional anisotropy, and eigenvalues. These diffusion parameters were examined as early markers for disease progression by relating them to clinical outcome of 6-month progression-free survival. The results indicated that changes from mid- to post-RT were significantly different between patients who progressed within 6 months vs those who were free of progression for 6 months after initiation of therapy. The study also showed that the changes in diffusion parameters from the mid- to post-RT scan may be more significant than those from pre- to mid-RT and pre- to post-RT. This is important because the mid-RT scan is currently not performed as part of the standard clinical care.

Keywords: apparent diffusion coefficient, diffusion-weighted imaging, disease progression, fractional anisotropy, glioblastoma multiforme.

Despite decades of research and development in the field of glioma treatment, little progress has been made in the overall survival of patients with glioblastoma multiforme (GBM), especially in patients aged 65 years and older.[1,2] Given the short survival time of GBM, the ability to assess early disease progression would enable early treatment termination, prevent additional unnecessary toxicity, and allow for prompt changes in treatment for nonresponding patients.

An assessment of disease progression is currently performed using the Macdonald criteria[3] based on serial MRI, which involves the monitoring of measurable changes in the anatomically contrast-enhancing lesion (CEL). For newly diagnosed patients, imaging anatomical assessment of chemo-radiotherapy is performed at the end of radiation therapy (RT), typically 2–3 months after the surgical diagnosis, and then Q2 months. A new class of antiangiogenic agents administered concurrent and adjuvant to RT with the standard of care temozolomide (TMZ) therapy can affect the growth of neoplastic blood vessels and result in the elimination of the contrast-enhancing volume, therefore making it difficult to perform an accurate imaging assessment of treatment efficacy. In many cases, it has been observed that although the original contrast-enhancing volume decreases or diminishes, new enhancing and/or nonenhancing regions of tumor appear.[4,5] This indicates that the contrast-enhancing component of the tumor does not encompass all of the biologically and clinically relevant disease. Therefore, finding an early imaging biomarker for disease progression may be important in determining treatment efficacy.

Diffusion tensor imaging is a noninvasive technique that allows for the probing and quantification of the

structure of biologic tissue at a microscopic level by measuring the Brownian motion of water molecules. Microscopic molecular movement of water in tumor tissue reflects tissue properties that include varying levels of structural alterations, tumor cellularity, and vasogenic edema. Diffusion imaging is hypothesized to detect early changes in morphology and physiology of tissues associated with water content. An increase in the apparent diffusion coefficient (ADC) may be due to changes in the permeability of cell membranes, cell swelling, and cell lysis, as well as the breakdown of cellular membranes and a reduction in cell density shortly after successful treatment.[6]

The ADC and the functional diffusion map (fDM) analysis have been reported as predictors of response to therapy in human brain tumors.[7–12] Studies suggest that both pretreatment ADC[8] and the change in ADC[11,12] are the predictors of response in brain tumors. Additionally, Mardor et al.[7] showed decreased ADC values in 3 patients with recurrent glioma who underwent imaging during the days of receiving convection-enhanced delivery of paclitaxel, whereas the corresponding increases in signal intensity of diffusion-weighted images were seen in a group of 15 patients undergoing the same treatment.[13]

Recent studies suggest that brain tumors that have responded favorably to RT or chemotherapy show an increase in the ADC values shortly after treatment, possibly representing an increase in the extracellular space; whereas a decrease in the ADC values suggests progression of disease as a result of an increase in tumor cells.[8,10,14]

The purpose of this study was to evaluate diffusion parameters within both the CEL and nonenhancing lesion for pre-, mid-, and post-RT scans in postsurgical GBM patients and examine whether the changes in these imaging parameters may serve as early markers for disease progression. Ultimately, the goal of treatment is to improve survival. However, trials based on overall survival as the primary endpoint for efficacy generally require longer follow-up time and are likely to be subject to potential confounding due to subsequent anticancer treatment after disease progression. In this paper, we use 6-month progression-free survival (6-moPFS) as the clinical endpoint of efficacy. 6-moPFS has been shown to be a strong predictor of survival and an important clinical endpoint in evaluating therapy for newly diagnosed or recurrent GBM patients.[15,16]

Materials and Methods

Study Population

A total of 49 newly diagnosed patients with GBMs who received surgery and were treated with the standard of care RT concurrently with TMZ and an adjuvant antiangiogenic drug followed by adjuvant plus TMZ and the antiangiogenic drug were included in this study. Patients were scanned within a week prior to treatment (pre-RT), between 3 and 5 weeks into treatment (mid-RT) and within 2 weeks after completion of RT (post-RT). Of the 49 patients, 2 patients withdrew within 1 month of starting treatment, 1 patient went off treatment at 3 months due to an infection, and 9 patients were not included due to not having pre-RT and mid- or post-RT scans. Of the 37 patients, 26 had all 3 (pre-, mid-, and post-RT scans), 9 had only pre- and post-RT scans, and 2 had pre- and mid-RT scans only.

The 37 patients (10 female and 27 male) included in the study ranged in age from 25 to 80, with a median of 56 years. Diagnosis was based on histologic examination using criteria defined by the World Health Organization (WHO). Patients provided informed consent as approved by the Committee on Human Research at our institution.

Treatment started <5 weeks after diagnosis, with fractionated RT with a total of 60 Gy being given over 6 weeks and TMZ 75 mg/m^2 being given daily during RT and then adjuvantly at 200 mg/m^2 on days 1–5 of a 28-day cycle. A protein kinase C-β inhibitor that is thought to have both antiproliferative and antiangiogenic properties was also given daily during RT and adjuvantly.[17,18] Twelve adjuvant cycles (1 cycle = 28 days) were planned.

Progression was assessed based on the Macdonald criteria[3] in combination with clinical information. Patients were grouped based on progression information assessed at 6 months from the pre-RT MR scan (typically within 2 weeks of initiation of RT; 6-moPFS): 19 patients showed progression (progressors) and 18 patients showed no progression (nonprogressors) by 6 months. To allow for variability in MRI scheduling, 6-moPFS was based on the progression status up to 200 days.

Conventional MRI

MR exams were performed with a 3T GE Signa Echospeed scanner (GE Healthcare Technologies). The MRI examination included axial T1-weighted pre- and post- gadolinium 3-dimensional inversion recovery spoiled gradient echo (IRSPGR) images (TR = 8 milliseconds, TE = 3 milliseconds, TI = 400 milliseconds, slice thickness = 1.5 mm, matrix = 256 × 256, FOV = 241 × 241 mm^2, flip angle = 15°) and axial T2-weighted fluid-attenuated inversion recovery (FLAIR) (TR = 9500 milliseconds, TE = 122 milliseconds, TI = 2375 milliseconds, slice thickness = 3 mm, matrix = 256 × 256, FOV = 241 × 241 mm^2). After each examination, the images were transferred to a SUN Ultra 10 workstation (Sun Microsystems) for postprocessing.

Diffusion-Weighted Imaging

Patients were scanned with 6 directional diffusion tensor echo-planar imaging sequence (TR = 7000 milliseconds, TE = 63 milliseconds, matrix size = 256 × 256, slice thickness = 3 mm, b = 1000 s/mm^2, FOV = 220 × 220 mm^2, NEX = 4). The eigenvalues (EV1–3),
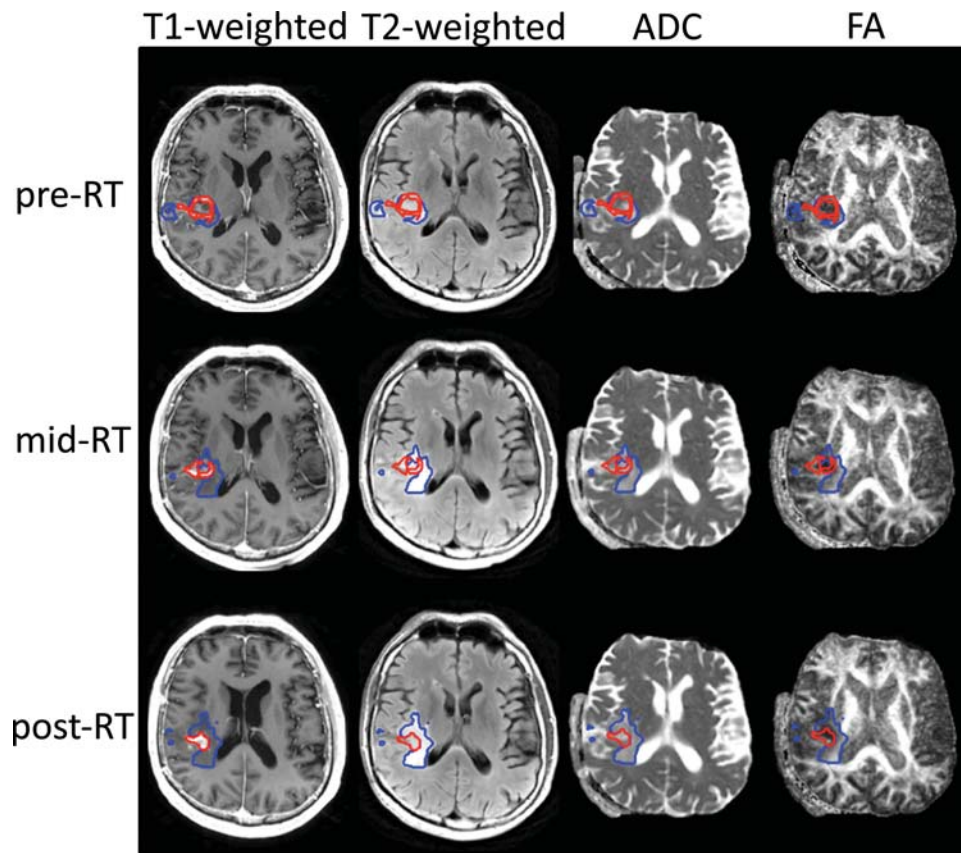
Fig. 1. First, pre-RT T2- aligned to T1-weighted images. Next, T2 from diffusion imaging aligned to T2-weighted image and applied to diffusion maps (eg, ADC and FA). Aligning the individual pregadolinium T1-weighted images then aligns the mid- and post-RT scans to the pre-RT scans. Finally, apply the previous individual mid- and post-RT transformation to all the images at that time point (eg, FLAIR, ADC, and FA). The NEL (blue) and CEL (red) are shown for the individual scan time points.

ADC, fractional anisotropy (FA), and the 3 eigenvalue maps (EV1, EV2, and EV3) were calculated on a pixel-by-pixel basis using software developed in-house, based on published algorithms.[19] The ADC, FA, EV1, EV2, and EV3 maps were registered to anatomical imaging by rigidly aligning the T2-weighted ($b = 0$) diffusion image to the T2-weighted FLAIR and applying the transformation to the ADC, FA, EV1, EV2, and EV3 maps[20] (Fig. 1).

Data Processing

The FLAIR and pregadolinium IRSPGR images were aligned to the postgadolinium IRSPGR using software developed in our laboratory.[21] An in-house semi-automated segmentation method was used to define the CEL on the postgadolinium T1-weighted IRSPGR image.[22] The T2 hyperintense region (T2ALL) was contoured on the T2-weighted FLAIR image. The nonenhancing lesion (NEL) was defined as T2ALL minus the CEL (T2ALL − CEL). Normalized ADC maps (nADC) were generated by dividing the ADC maps by the median ADC value within the normal-appearing white matter mask, which was segmented using VTK FAST (FMRIB's Automated Segmentation Tool)

Software on the pregadolinium T1-weighted IRSPGR image.[23] The same method was applied to the FA, EV1, EV2, and EV3 maps to generate normalized FA (nFA), normalized EV1 (nEV1), nEV2, and nEV3 maps.

Statistical Analysis

Summary statistics are provided as medians and ranges. The volumes and median normalized diffusion parameters (ie, nADC, nFA, nEV1, nEV2, and nEV3) were calculated within the CEL, NEL, and T2ALL regions. The percent change for each volume and median normalized diffusion parameter was calculated for 3 time point changes: from pre- to mid-RT (pre−mid), as $100 \times$ [mid − pre]/pre; from mid- to post-RT (mid−post), as $100 \times$ [post − mid]/mid; and from pre- to post-RT (pre−post), as $100 \times$ [post − pre]/pre within the CEL, NEL, and T2ALL regions. Differences in the imaging parameters between progressors and nonprogressors were assessed using a 2-sided Mann–Whitney rank-sum test for volumes, median values, and percent changes to examine whether the values of the imaging markers at a given time point or the early changes in these markers predicted 6-month progression status. The changes (pre−mid, mid−post, and pre−post) were assessed for

Table 1. Median (range) of the pre-, mid-, and post-RT and the median (range) percent change from pre- to mid-, mid- to post-, and pre- to post-RT volumes within the CEL, NEL, and T2ALL for all patients (ALL), progressors (P), and nonprogressors (NP), along with the Mann−Whitney rank-sum P-value of the P vs NP

	Volume (cc)					
	Pre	Mid	Post	Pre to mid	Mid to post	Pre to post
CEL						
ALL	5.44 (0−44)	2.96 (0−19)	3.14 (0−20)	−56% (−100 to 476)	−14% (−100 to 163)	−52% (−100 to 1869)
P	6.37 (0−21)	4.17 (0−19)	5.01 (0−20)	−30% (−100 to 62)	49% (−100 to 163)	−11% (−100 to 153)
NP	4.38 (0−44)	2.25 (0−13)	1.51 (0−19)	−58% (−100 to 476)	−35% (−90 to 72)	−67% (−99 to 1869)
Rank sum	.1325	.1943	.0144*	.4363	.0121*	.2079
NEL						
ALL	14.43 (1−98)	12.01 (0−77)	15.55 (0−145)	−32% (−100 to 271)	20% (−100 to 758)	−0% (−100 to 1690)
P	21.90 (1−98)	15.11 (0−64)	18.12 (0−145)	−31% (−100 to 271)	65% (−100 to 758)	25% (−100 to 1690)
NP	14.15 (1−86)	11.77 (0−77)	12.77 (1−66)	−32% (−100 to 149)	6% (−67 to 155)	−8% (−80 to 256)
Rank sum	.4384	.2458	.0832	.669	.2849	.1668
T2ALL						
ALL	24.29 (1−105)	16.13 (0−78)	19.56 (0−148)	−36% (−100 to 231)	19% (−100 to 361)	−0% (−100 to 324)
P	31.42 (6−105)	23.93 (0−74)	25.73 (0−148)	−29% (−100 to 74)	62% (−100 to 361)	31% (−100 to 324)
NP	20.71 (1−88)	14.65 (0−78)	17.13 (1−67)	−37% (−100 to 231)	−7% (−67 to 72)	−32% (−82 to 138)
Rank sum	.2545	.1268	.066	.5413	.0701	.1249

*P<0.05; volume/Post/CEL/Ranksum 0.0144 value.

significance within each group (progressors and nonprogressors) using a 2-sided Wilcoxon signed-rank test. Owing to the exploratory nature of these analyses, there was no adjustment for multiple comparisons and a P-value <.05 was used to indicate statistical significance.

The procedures described by Moffat et al.[24] for calculating fDMs were also evaluated. These involve the identification of overlapping regions of interest on the pre- and mid-RT scans. The recommended minimum overlapping CEL volume that should be considered for this technique is 4 cc.[25] The next step is to generate the percent volume of the overlapping region that shows increases in the ADC value (V_R) or decreases in the ADC value (V_B) of more than or less than 550×10^{-6} mm^2/s, respectively. The remaining percentage of overlapping volume is referred to as V_G. For lesions that satisfy the criteria defined above, the differences in V_R and V_B between patients who progress vs those who do not may be evaluated using a Mann−Whitney rank-sum test.

Results

Volume

Three patients received a biopsy, whereas 10 patients received a gross-total resection and 24 patients received a subtotal resection of the CEL. The median volumes (cc) within the CEL, NEL, and T2ALL for the pre-, mid-, and post-RT are presented in Table 1. The region of overlap between the pre- and mid-RT CEL, NEL, and T2ALL volumes had a median (range) of 1.32 (0−13.68), 3.89 (0−67.41), and 8.61 (0−68.55) cc, respectively. This is significantly smaller than the individual pre- and mid-RT volumes within the CEL, NEL, and T2ALL volumes (Table 1). Visual

inspection indicated that this was primarily due to there being tissue shift between successive examinations.

The CEL volume was significantly higher (P = .0144) at the post-RT scan with a median of 5.01 cc for progressors and 1.51 cc for nonprogressors. The change in CEL volume from mid- to post-RT was also significantly different (P = .0121) between progressors (with a median increase of 49%) and nonprogressors (with a median decrease of 35%) (Fig. 2). No differences in the volumes or percent changes within the NEL and T2ALL regions were noted between progressors and nonprogressors for any of the time points. The Wilcoxon signed-rank test showed a significant change from pre- to mid-RT within the CEL, NEL, and T2ALL.

Normalized Apparent Diffusion Coefficient (nADC)

The distribution of median nADC values within the CEL for the pre-, mid-, and post-RT scans is presented in Fig. 3. Mid-RT median nADC values within the CEL showed a trend (P = .073) toward higher values for nonprogressors, median (range) of 1.69 (1.31 to 1.98), relative to the progressors, 1.53 (0.97 to 1.93). No significant changes were noted between progressors and nonprogressors for any time point within the NEL or T2ALL (Table 2).

The percent change in the nADC from mid- to post-RT showed significant differences between progressors and nonprogressors within CEL (P = .0221), NEL (P = .0192), and T2ALL (P = .0069). Significantly higher percent changes were observed within the CEL, NEL, and T2ALL for progressors (16%, 13%, and 14%) vs nonprogressors (4%, 3%, and 3%).

Within the CEL, the median percent change in nADC (P-value from the Wilcoxon signed-rank test) for
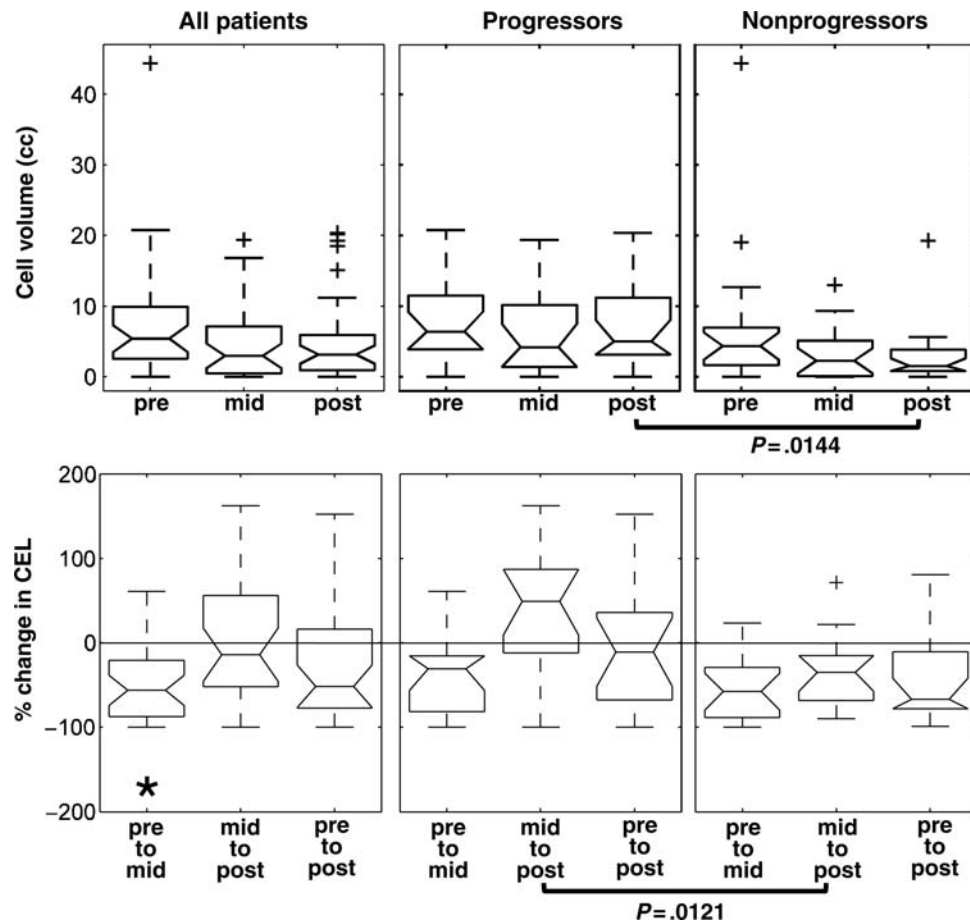
Fig. 2. CEL volume and percent change in CEL for all patients, progressors, and nonprogressors. Progressors showed significantly higher CEL volumes at post-RT and significantly higher percent changes of CEL volume from mid- to post-RT (P-values presented are based on the 2-sided Mann–Whitney rank-sum test). Changes between 2 time points within each patient group were tested using the Wilcoxon signed-rank test; statistically significant (P<0.05) changes were noted with an asterisk; + sign represents the boxplot outliers.

progressors and nonprogressors was 2% ($P = .2266$) and 14% ($P = .0419$) from pre- to mid-RT, and 16% ($P = .0005$) and 4% ($P = .1418$) from mid- to post-RT. This suggests that progressors showed a significant median nADC change from mid- to post-RT, whereas nonprogressors showed a significant change from pre- to mid-RT. Within the NEL and T2ALL, progressors showed a significant percent increase of 13% ($P = .041$) and 14% ($P = .001$) respectively, in the median nADC values from mid- to post-RT.

Normalized Fractional Anisotropy (nFA)

No significant differences were observed for the median nFA values between progressors and nonprogressors for any of the time points (pre-, mid-, or post-RT) within any of the regions (CEL, NEL, or T2ALL). The percent change in nFA from mid- to post-RT within the CEL and NEL was significant ($P = .0396$ and .0421, respectively) with larger percent decreases in progressors (-13% and -9%) vs nonprogressors (-5% and -2%), respectively (Table 3). Progressors showed a significant change in median nFA values within the

CEL from mid- to post-RT ($P = .001$) with no significant differences within the NEL or T2ALL region.

Normalized Eigenvalues (nEV1–3)

Nonprogressors vs. progressors showed significantly higher mid-RT CEL nEV1 values, 1.39 vs 1.28 ($P = .037$), and nEV2 values, 1.77 vs 1.64 ($P = .0432$). This difference was not observed within the NEL and T2ALL. Percent changes in the nEV1–3 values between progressors vs nonprogressors showed trends toward different percent changes from mid- to post-RT within all the regions, with significantly different nEV3 percent changes within the NEL ($P = .0069$) and T2ALL ($P = .0051$). Similar to the nADC, more significant P-values were observed in the Wilcoxon signed-rank test of the nEV1–3 values from mid- to post-RT for progressors vs nonprogressors within all the regions.

fDM Parameters

Using the 4 cc cutoff for intersecting volumes would have allowed only 5 of 28 patients with a median (range) intersecting volume of pre- to mid-RT CEL of
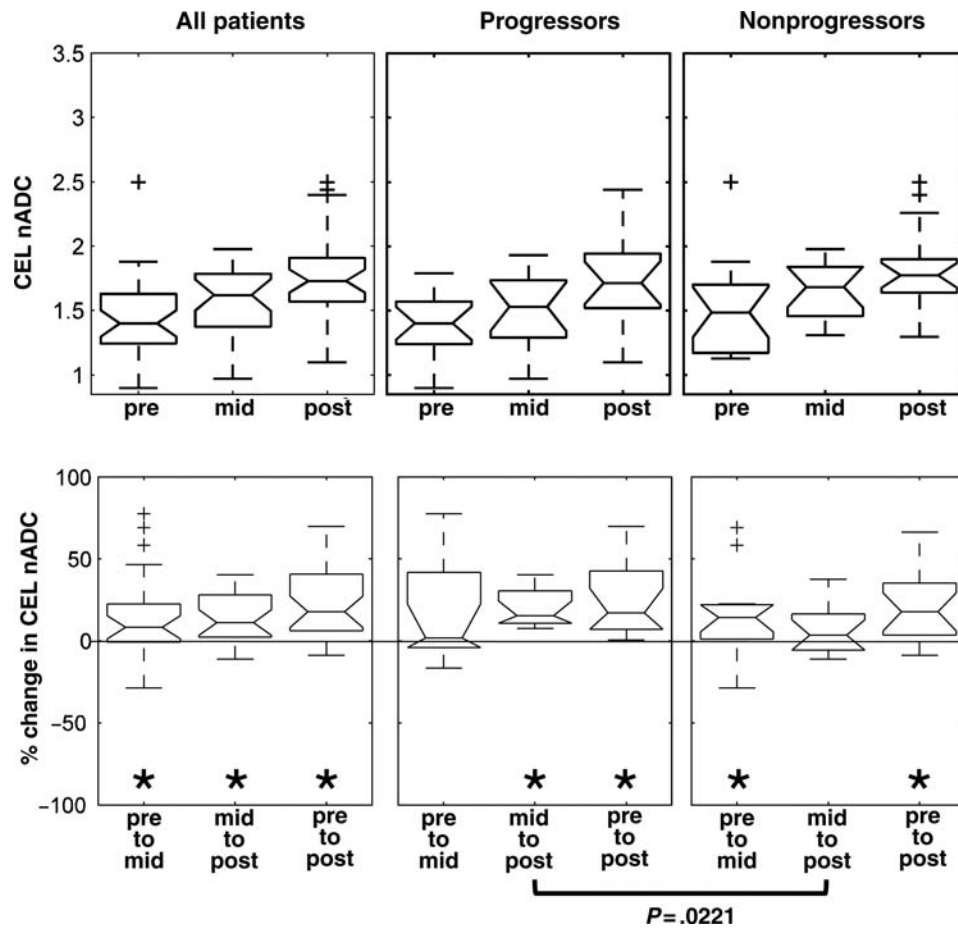
Fig. 3. A trend of increasing CEL nADC values was observed over time. A trend toward significantly different percent change from mid- to post-RT scans was observed between progressors and nonprogressors (*P*-values presented are based on the 2-sided Mann–Whitney rank-sum test). Changes between 2 time points within each patient group were tested using the Wilcoxon signed-rank test; statistically significant (*P*<0.05) changes were noted with an asterisk; + sign represents the box plot outliers.

6.12 cc (4.08 to 13.68 cc). Comparison of the fDM parameters within the CEL regions irrespective of their size showed that there was no significant difference in V_R or V_B percentages between progressors and nonprogressors from pre- to mid-RT or pre- to post-RT. Similar results were obtained when the NEL or T2ALL regions were used as the basis for the analysis rather than the CEL.

Discussion

GBMs are histologically, radiographically, and clinically heterogeneous. On average, 50% of these patients respond to the current standard of care, which is concurrent radiation and chemotherapy.[26] As new agents that work on specific molecular and genetic targets are integrated with the standard of care, it is extremely important to assess response to treatment as early as possible in the course of treatment. This is especially true with new antiangiogenic agents that can significantly affect the contrast-enhancing volume within 24 hours, a time scale very likely affecting the integrity of the blood–brain barrier and not tumor burden. Therefore, the

contrast enhancement may no longer be considered a good measure of tumor burden for these therapies.[4,5]

Other parameters that have recently been suggested as being relevant as early biomarkers for predicting subsequent progression are the mean, median, and histogram analysis of the ADC and the manner in which these parameters change before and during treatment.[7–12,27] In this study, we evaluated the diffusion parameters in relation to 6-moPFS within the whole tumor, and the contrast enhancement and nonenhancement for pre-, mid-, and post-RT scans.

The median normalized ADC values within the contrast enhancement at the mid-RT exam showed a trend toward higher values for the nonprogressors. Prior studies that included a mix of grade III and IV gliomas along with metastatic brain tumors have suggested that an increase in the ADC preceded tumor response,[7,8,10] but these studies assessed the ADC weeks post-treatment. Tomura et al.[11] showed that the normalized ADC values of primarily metastatic tumors were significantly higher at 2–4 weeks after stereotactic irradiation when compared with the baseline scan. There was a significant difference in the normalized ADC values at 2–4

Table 2. Median (range) of the pre-, mid-, and post-RT and the median (range) percent change from pre- to mid-, mid- to post-, and pre- to post-RT median nADC within the CEL, NEL, and T2ALL volumes for all patients (ALL), progressors (P), and nonprogressors (NP), along with the Mann–Whitney rank-sum P-value of the P vs NP

	nADC			Percent change in nADC		
	Pre	Mid	Post	Pre to mid	Mid to post	Pre to post
CEL						
ALL	1.40 (0.29–2.50)	1.62 (0.97–1.98)	1.73 (1.10–2.50)	8% (−29 to 78)	11% (−11 to 40)	18% (−9 to 466)
P	1.40 (0.90–1.79)	1.53 (0.97–1.93)	1.71 (1.10–2.44)	2% (−16 to 78)	16% (8–40)	17% (1–133)
NP	1.48 (0.29–2.50)	1.69 (1.31–1.98)	1.77 (1.30–2.50)	14% (−29 to 69)	4% (−11 to 38)	18% (−9 to 466)
Rank sum	.4475	.073	.49	.6251	.0221*	.69
NEL						
ALL	1.42 (1.02–3.38)	1.45 (1.03–2.18)	1.50 (1.07–1.94)	−1% (−67 to 41)	7% (−17 to 19)	5% (−68 to 52)
P	1.48 (1.02–2.19)	1.44 (1.03–2.18)	1.52 (1.17–1.94)	−2% (−33 to 41)	13% (−17 to 19)	3% (−24 to 52)
NP	1.36 (1.24–3.38)	1.49 (1.10–1.77)	1.47 (1.07–1.82)	1% (−67 to 33)	3% (−13 to 18)	5% (−68 to 41)
Rank sum	.7496	.2599	.6074	.7652	.0192*	.8555
T2ALL						
ALL	1.40 (0.94–2.46)	1.48 (1.02–1.76)	1.55 (1.08–1.94)	1% (−54 to 53)	8% (−9 to 25)	4% (−56 to 66)
P	1.41 (0.94–1.94)	1.42 (1.02–1.76)	1.56 (1.17–1.94)	1% (−25 to 53)	14% (−0 to 25)	9% (−8 to 66)
NP	1.37 (1.26–2.46)	1.49 (1.14–1.76)	1.51 (1.08–1.84)	−1% (−54 to 37)	3% (−9 to 15)	3% (−56 to 46)
Rank sum	.8553	.3823	.446	.8362	.0069*	.5184

*$P<0.05$; percent change in nADC/mid to post/T2ALL/Ranksum 0.0069.

Table 3. Median (range) of the pre-, mid-, and post-RT and the median (range) percent change from pre- to mid-, mid- to post-, and pre- to post-RT median nFA within the CEL, NEL, and T2ALL volumes for all patients (ALL), progressors (P), and nonprogressors (NP), along with the Mann–Whitney rank-sum P-value of the P vs NP

	nFA			Percent change in nFA		
	Pre	Mid	Post	Pre to mid	Mid to post	Pre to post
CEL						
ALL	0.46 (0.16–1.02)	0.46 (0.29–0.72)	0.46 (0.26–0.92)	−1% (−42 to 97)	−7% (−36 to 35)	1% (−61 to 156)
P	0.46 (0.34–1.02)	0.46 (0.29–0.67)	0.43 (0.26–0.74)	−9% (−42 to 26)	−13% (−32 to 0)	−11% (−61 to 24)
NP	0.42 (0.16–0.79)	0.53 (0.32–0.72)	0.47 (0.33–0.92)	1% (−16 to 97)	−5% (−36 to 35)	7% (−22 to 156)
Rank sum	.2269	.2409	.4171	.2268	.0396*	.0575
NEL						
ALL	0.48 (0.17–0.92)	0.54 (0.31–0.84)	0.52 (0.36–0.77)	6% (−47 to 224)	−5% (−22 to 60)	8% (−50 to 200)
P	0.49 (0.21–0.92)	0.56 (0.31–0.84)	0.53 (0.36–0.77)	6% (−47 to 91)	−9% (−22 to 35)	13% (−50 to 133)
NP	0.48 (0.17–0.72)	0.51 (0.39–0.64)	0.52 (0.38–0.69)	5% (−31 to 224)	−2% (−17 to 60)	3% (−32 to 200)
Rank sum	1	.0886	.9076	.9085	.0421*	.8296
T2ALL						
ALL	0.46 (0.26–0.98)	0.52 (0.36–0.81)	0.50 (0.33–0.77)	5% (−50 to 92)	−5% (−28 to 50)	7% (−53 to 92)
P	0.46 (0.27–0.98)	0.53 (0.36–0.81)	0.48 (0.33–0.77)	−1% (−50 to 73)	−11% (−28 to 26)	6% (−53 to 78)
NP	0.47 (0.26–0.71)	0.51 (0.38–0.66)	0.51 (0.38–0.68)	9% (−24 to 92)	−2% (−18 to 50)	8% (−29 to 92)
Rank sum	.8077	.6616	.5726	.6458	.0604	.5623

*$P<0.05$; percent change in nFA/mid to post/CEL&NEL/Ranksum .0396 and .0421.

weeks after stereotactic irradiation between the responder and the nonresponder groups ($P < .05$) when evaluated at 8–12 weeks but not at 2–4 weeks after stereotactic irradiation. We also observed significantly higher normalized ADC values from pre- to post-RT ($P < .0001$) for progressors and nonprogressors. We did not observe significant differences in post-RT normalized ADC values between progressors vs nonprogressors within any of the regions. However, there was a

trend toward higher mid-RT normalized ADC, EV1, and EV2 values among nonprogressors compared with progressors.

The within-patient analysis that was performed in our population indicated that progressors showed a significant change in normalized ADC from mid- to post-RT and pre- to post-RT, whereas the nonprogressors showed a significant change from pre- to mid-RT and pre- to post-RT. This could explain why the percent

change in the normalized ADC from mid- to post-RT showed much clearer significant difference between progressors and nonprogressors within all the regions, with significantly higher percent changes for progressors vs nonprogressors. Previous studies have shown dynamic changes in the ADC after treatment,[7,10] with ADC values increasing and then decreasing again. In this study, we noticed dynamic changes (increases, decreases, and stability) in the normalized ADC between pre- to mid-RT and mid- to post-RT, with the changes from mid- to post-RT seeming to indicate the most significant separation between progressors and nonprogressors. This suggests that an increase or decrease in the ADC alone is not sufficient to determine treatment response and that the timing of these increases and/or decreases may be very important both during and after treatment. For the treatment considered in this study, it appears that the percent changes in the ADC from mid- to post-RT are significant in assessing 6-moPFS.

The majority of patients were off steroids or tapering down. The literature suggests variable effects of high steroid dose on ADC values. Sinha et al.[28] showed an increase in the ADC values within a nonenhancing lesion of a patient. Sinha et al. also showed a decrease in the ADC values within the nonenhancing lesions,[29–31] whereas Minamikawa et al. showed no significant decrease within the nonenhancing lesions.[32] Most studies suggest a decease in the ADC values within enhancing lesions of 6%–11%.[30,31] Since the majority of patients were off steroids or tapering down, we suspect that steroid use would not have a strong impact on the ADC values in this study.

Key to the interpretation of the fDM parameters is a comparison between parameters in similar regions of tissue in the pretreatment and follow-up scans. This can be problematic when there is an extensive surgical resection that leaves a relatively small region of residual tumor, which may lead to substantial tissue shift in the follow-up examinations. In this study, most patients received sub- or gross-total resections. This translated to a median intersecting pre- and mid-RT contrast enhancement of 1.3 cc. For the majority of patients, the residual contrast enhancement appeared as a narrow region that surrounded the cavity and temporal changes led to substantial tissue shift for follow-up examinations. For cases where the region is relatively small, it is difficult to make accurate correlations between parameter values from different examinations. It is for this reason that requiring the patient to have a minimum volume of intersecting contrast enhancement

of 4 cc was recently proposed as a criterion for eligibility to apply the fDM technique.[25] The fact that our lesion volumes were mostly at the threshold or lower than the suggested limit means that it is not surprising that there was no significant difference in the V_R or V_B parameters between the progressors and nonprogressors.

In conclusion, this study assessed the changes in the volumes and diffusion parameters within the enhancing and nonenhancing lesions at pre-, mid-, and post-RT and how these changes may relate to the clinical outcome of 6-moPFS. The results indicated that changes from mid- to post-RT were significantly different between patients who progressed within 6 months vs those who were free of progression for 6 months after initiation of therapy. The study also showed that changes in diffusion parameters from the mid- to post-RT scan may be more significant than changes from pre- to mid-RT or from pre- to post-RT. This is important because the mid-RT scan is currently not performed as part of the standard clinical care. Although we initially intended to apply the fDM method to evaluate our patients, the fact that the median intersecting pre- and mid-RT CEL volume was 1.3 cc meant that our data did not satisfy the requirement of a minimum volume of 4 cc. Our observation of no significant differences in fDM parameters was consistent with the observation that, in its current form, the technique is unable to assess response to therapy in populations of patients with GBM who have had resections that leave behind limited or no residual contrast enhancement.

Acknowledgements

Funding

References

1. Wrensch M, Minn Y, Chew T, Bondy M, Berger MS. Epidemiology of primary brain tumors: current concepts and review of the literature. *Neurooncology*. 2002;4:278–299.

2. Legler JM, Ries LA, Smith MA, et al. Cancer surveillance series [corrected]: brain and other central nervous system cancers: recent trends in incidence and mortality. *J Natl Cancer Inst*. 1999;91:1382–1390.

3. Macdonald DR, Cascino TL, Schold SC, Jr, Cairncross JG. Response criteria for phase II studies of supratentorial malignant glioma. *J Clin Oncol*. 1990;8:1277–1280.

4. van den Bent MJ, Vogelbaum MA, Wen PY, Macdonald DR, Chang SM. End point assessment in gliomas: novel treatments limit usefulness of classical Macdonald's criteria. *J Clin Oncol*. 2009;27: 2905–2908.

5. Wong ET, Brem S. Taming glioblastoma: targeting angiogenesis. *J Clin Oncol*. 2007;25:4705–4706.

6. Hamstra DA, Rehemtulla A, Ross BD. Diffusion magnetic resonance imaging: a biomarker for treatment response in oncology. *J Clin Oncol*. 2007;25:4104–4109.

7. Mardor Y, Roth Y, Lidar Z, et al. Monitoring response to convection-enhanced taxol delivery in brain tumor patients using diffusion-weighted magnetic resonance imaging. *Cancer Res*. 2001;61:4971–4973.

8. Mardor Y, Pfeffer R, Spiegelmann R, et al. Early detection of response to radiation therapy in patients with brain malignancies using conventional and high b-value diffusion-weighted magnetic resonance imaging. *J Clin Oncol*. 2003;21:1094–1100.

9. Hamstra DA, Chenevert TL, Moffat BA, et al. Evaluation of the functional diffusion map as an early biomarker of time-to-progression and overall survival in high-grade glioma. *Proc Natl Acad Sci USA*. 2005;102:16759–16764.

10. Chenevert TL, Stegman LD, Taylor JM, et al. Diffusion magnetic resonance imaging: an early surrogate marker of therapeutic efficacy in brain tumors. *J Natl Cancer Inst*. 2000;92:2029–2036.

11. Tomura N, Narita K, Izumi J, et al. Diffusion changes in a tumor and peritumoral tissue after stereotactic irradiation for brain tumors: possible prediction of treatment response. *J Comput Assist Tomogr*. 2006;30: 496–500.

12. Schubert MI, Wilke M, Muller-Weihrich S, Auer DP. Diffusion-weighted magnetic resonance imaging of treatment-associated changes in recurrent and residual medulloblastoma: preliminary observations in three children. *Acta Radiol*. 2006;47:1100–1104.

13. Lidar Z, Mardor Y, Jonas T, et al. Convection-enhanced delivery of paclitaxel for the treatment of recurrent malignant glioma: a phase I/II clinical study. *J Neurosurg*. 2004;100:472–479.

14. Chenevert TL, McKeever PE, Ross BD. Monitoring early response of experimental brain tumors to therapy using diffusion magnetic resonance imaging. *Clin Cancer Res*. 1997;3:1457–1466.

15. Lamborn KR, Yung WK, Chang SM, et al. Progression-free survival: an important end point in evaluating therapy for recurrent high-grade gliomas. *Neurooncology*. 2008;10:162–170.

16. Polley MC, Lamborn KR, Chang S, et al. Six-month progression-free survival as an alternative primary efficacy endpoint to overall survival in newly-diagnosed glioblastoma patients receiving temozolomide. *Neurooncology*. 2009.

17. Teicher BA, Menon K, Alvarez E, et al. Antiangiogenic and antitumor effects of a protein kinase Cbeta inhibitor in human T98G glioblastoma multiforme xenografts. *Clin Cancer Res*. 2001;7:634–640.

18. Aeder SE, Martin PM, Soh JW, Hussaini IM. PKC-eta mediates glioblastoma cell proliferation through the Akt and mTOR signaling pathways. *Oncogene*. 2004;23:9062–9069.

19. Basser PJ, Pierpaoli C. Microstructural and physiological features of tissues elucidated by quantitative-diffusion-tensor MRI. *J Magn Reson B*. 1996;111:209–219.

20. Hartkens T, Rueckert D, Schnabel JA, Hawkes DJ, Hill DLG. VTK CISG Registration Toolkit: An Open Source Software Package for Affine and Non-Rigid Registration of Single- and Multimodal 3D Images. BVM2002, Leipzig: Springer-Verlag; 2002.

21. Nelson SJ, Nalbandian AB, Proctor E, Vigneron DB. Registration of images from sequential MR studies of the brain. *J Magn Reson Imaging*. 1994;4:877–883.

22. Saraswathy S, Crawford F, Nelson S. Semi-automated segmentation of brain tumor lesions in MR images (abstract 1609). Proceedings of the 14th Annual Meeting of ISMRM, Seattle, WA, USA, 2006.

23. Zhang Y, Brady M, Smith S. Segmentation of brain MR images through a hidden Markov random field model and the expectation-maximization algorithm. *IEEE Trans Med Imaging*. 2001;20:45–57.

24. Moffat BA, Chenevert TL, Lawrence TS, et al. Functional diffusion map: a noninvasive MRI biomarker for early stratification of clinical brain tumor response. *Proc Natl Acad Sci USA*. 2005;102:5524–5529.

25. Hamstra DA, Galban CJ, Meyer CR, et al. Functional diffusion map as an early imaging biomarker for high-grade glioma: correlation with conventional radiologic response and overall survival. *J Clin Oncol*. 2008;26:3387–3394.

26. Stupp R, Dietrich PY, Ostermann Kraljevic S, et al. Promising survival for patients with newly diagnosed glioblastoma multiforme treated with concomitant radiation plus temozolomide followed by adjuvant temozolomide. *J Clin Oncol*. 2002;20:1375–1382.

27. Pope WB, Kim HJ, Huo J, et al. Recurrent glioblastoma multiforme: ADC histogram analysis predicts response to bevacizumab treatment. *Radiology*. 2009;252:182–189.

28. Sinha S, Bastin ME, Whittle IR. Rapid clinical deterioration in a patient with multi-focal glioma despite corticosteroid therapy: a quantitative MRI study. *Br J Neurosurg*. 2003;17:537–540; discussion 540.

29. Sinha S, Bastin ME, Wardlaw JM, Armitage PA, Whittle IR. Effects of dexamethasone on peritumoural oedematous brain: a DT-MRI study. *J Neurol Neurosurg Psychiatry*. 2004;75:1632–1635.

30. Bastin ME, Carpenter TK, Armitage PA, et al. Effects of dexamethasone on cerebral perfusion and water diffusion in patients with high-grade glioma. *AJNR Am J Neuroradiol*. 2006;27:402–408.

31. Armitage PA, Schwindack C, Bastin ME, Whittle IR. Quantitative assessment of intracranial tumor response to dexamethasone using diffusion, perfusion and permeability magnetic resonance imaging. *Magn Reson Imaging*. 2007;25:303–310.

32. Minamikawa S, Kono K, Nakayama K, et al. Glucocorticoid treatment of brain tumor patients: changes of apparent diffusion coefficient values measured by MR diffusion imaging. *Neuroradiology*. 2004;46:805–811.